

Effects of Drug Loading on the Antitumor Activity of a Monoclonal Antibody Drug Conjugate

Kevin J. Hamblett, Peter D. Senter, Dana F. Chace, Michael M. C. Sun, Joel Lenox, Charles G. Cerweny, Kim M. Kissler, Starr X. Bernhardt, Anastasia K. Kopcha, Roger F. Zabinski, Damon L. Meyer, and Joseph A. Francisco

Seattle Genetics, Inc., Bothell, Washington

ABSTRACT

Purpose: An antibody-drug conjugate consisting of monomethyl auristatin E (MMAE) conjugated to the anti-CD30 monoclonal antibody (mAb) cAC10, with eight drug moieties per mAb, was previously shown to have potent cytotoxic activity against CD30⁺ malignant cells. To determine the effect of drug loading on antibody-drug conjugate therapeutic potential, we assessed cAC10 antibody-drug conjugates containing different drug-mAb ratios *in vitro* and *in vivo*.

Experimental Design: Coupling MMAE to the cysteines that comprise the interchain disulfides of cAC10 created an antibody-drug conjugate population, which was purified using hydrophobic interaction chromatography to yield antibody-drug conjugates with two, four, and eight drugs per antibody (E2, E4, and E8, respectively). Antibody-drug conjugate potency was tested *in vitro* against CD30⁺ lines followed by *in vivo* xenograft models. The maximum-tolerated dose and pharmacokinetic profiles of the antibody-drug conjugates were investigated in mice.

Results: Although antibody-drug conjugate potency *in vitro* was directly dependent on drug loading (IC₅₀ values E8 < E4 < E2), the *in vivo* antitumor activity of E4 was comparable with E8 at equal mAb doses, although the E4 contained half the amount of MMAE per mAb. E2 was also an active antitumor agent but required higher doses. The maximum-tolerated dose of E2 in mice was at least double that of E4, which in turn was twice that of E8. MMAE loading affected plasma clearance, as E8 cleared 3-fold faster than E4 and 5-fold faster than E2.

Conclusions: By decreasing drug loading per antibody, the therapeutic index was increased demonstrating that

drug loading is a key design parameter for antibody-drug conjugates.

INTRODUCTION

Recent success in the development of monoclonal antibodies (mAbs) for the treatment of cancer, such as rituximab for the treatment of non-Hodgkin's B-cell lymphoma and trastuzumab for breast cancer (1), have proven that mAbs can be a valuable weapon in the battle against cancer. To further advance the use of mAb-based therapies for cancer, a number of novel approaches have been explored. For example several approaches have been shown to enhance the ability of an antibody to mediate antibody-dependent cell-mediated cytotoxicity by optimizing the structure of the Fc-associated N-linked oligosaccharide (2, 3). Alternatively, cell-killing payloads such as protein toxins (4), radionuclides (5, 6), and anticancer drugs (7–9) have been conjugated to mAbs to generate immunotoxins, radioimmunoconjugates, and antibody-drug conjugates, respectively.

Gemtuzumab ozogamicin, an antibody-drug conjugate that is composed of the potent DNA minor groove binder calicheamicin linked covalently to an anti-CD33 mAb (8), was approved in 2000 by the United States Food and Drug Administration for the treatment of patients with relapsed acute myeloid leukemia (10). Other antibody-drug conjugates currently in development use a number of different cytotoxic drugs and linkage systems. For example, the maytansine-derivative DM1, a potent antimicrotubule agent, is used in huN901-DM1 for small-cell lung cancer and huC242-DM1, which targets the CanAg antigen present on various tumors (9). SGN-15 is an anti-Lewis Y antibody conjugated to doxorubicin and is currently in a phase II trial for non-small-cell lung cancer (7). Several other antibody-drug conjugates have shown pronounced activities in preclinical models and are advancing toward or have entered clinical trials (11–15).

Development of antibody-drug conjugates with therapeutic potential involves the optimization of several critical parameters. These include the use of highly potent drugs that are attenuated and stable while attached to the mAbs (12–14, 16) and the use of drug-mAb linkers that allow for the release of active drug only when the mAb has reached the target site (12, 17–20). Another key factor is the choice of target antigen. The target antigen should internalize upon mAb binding, have high expression on tumor cells, and little to no expression on normal cells.

The antigen CD30 is highly expressed on the surface of cancer cells such as Hodgkin's disease (21) and anaplastic large cell lymphomas (22). This expression, coupled with limited expression on normal cells (21, 23, 24), makes CD30 an attractive target for antibody-drug conjugate therapy. We recently demonstrated that the chimeric mAb cAC10 has antitumor activity against Hodgkin's disease both *in vitro* and in s.c. and disseminated SCID mouse xenograft models (25). We subse-

Received 4/21/04; revised 7/12/04; accepted 7/13/04.

The costs of publication of this article were defrayed in part by the payment of page charges. This article must therefore be hereby marked *advertisement* in accordance with 18 U.S.C. Section 1734 solely to indicate this fact.

Requests for reprints: Joseph A. Francisco, Seattle Genetics, Inc., 21823 30th Drive Southeast, Bothell, WA 98021. Phone: (425) 527-4910; Fax: (425) 527-4609; E-mail: jfrancisco@seagen.com.

©2004 American Association for Cancer Research.

quently reported that the antitumor activity of cAC10 could be dramatically enhanced by generating antibody-drug conjugates with derivatives of the cytotoxic agent auristatin E as the drug component (12, 13). These antibody-drug conjugates were highly effective in murine xenograft models at well-tolerated doses.

In developing the cAC10 antibody-drug conjugate, emphasis was placed on the stability of the linker, the method by which the drug was covalently attached to the mAb, and optimizing the potency of the drug component. Historically, augmenting the potency of an antibody-drug conjugate involved increasing the number of drugs on an antibody (20) or conjugating more potent drugs (12). Although previous reports describe how drug loading influences *in vitro* characteristics (16, 20, 26), the effects of drug multiplicity on *in vivo* parameters of antibody-drug conjugates has not been described. In the present work, we have evaluated the effect of drug loading on the *in vitro* and *in vivo* properties of cAC10 antibody-drug conjugates. The characteristics of cAC10 loaded with different ratios of MMAE demonstrate how drug loading affects pharmacokinetics and the therapeutic index parameters of efficacy and toxicity, which reveals drug loading as an important design parameter of antibody-drug conjugates.

MATERIALS AND METHODS

Cells and Reagents. CD30-positive anaplastic large-cell lymphoma line Karpas-299 and CD30-negative WSU-NHL were obtained from the Deutsche Sammlung von Mikroorganismen und Zellkulturen GmbH (Braunschweig, Germany). L540cy, a derivative of the Hodgkin's disease line L540 adapted to xenograft growth, was developed by Dr. Harald Stein (Institut für Pathologie, University of Veinikum Benjamin Franklin, Berlin, Germany). Cell lines were grown in RPMI 1640 (Life Technologies, Inc., Gaithersburg, MD) supplemented with 10% fetal bovine serum.

Construction and Purification of cAC10-Val-Cit-MMAE Antibody-Drug Conjugates. The E8 antibody-drug conjugate was generated as described previously (12, 13). Briefly, cAC10 was mixed with DTT at 37°C for 30 minutes, and the buffer was exchanged by elution through Sephadex G-25 resin with PBS containing 1 mmol/L diethylenetriaminepentaacetic acid. PBS containing 1 mmol/L diethylenetriaminepentaacetic acid (PBS/D) was added to the reduced mAb (final concentration, 2.5 mg/mL). The thiol concentration was ~8.4 thiols/mAb as measured by Ellman's reagent, 5,5'-dithiobis(2-nitrobenzoic acid) [DTNB]. A 9.5-fold molar excess of maleimidocaproyl-Val-Cit-MMAE, subsequently referred to as Val-Cit-MMAE, was added to the reduced antibody at 4°C for 1 hour, and the conjugation reaction was quenched by adding a 20-fold excess of cysteine. The reaction mixture was concentrated by centrifugal ultrafiltration and buffer-exchanged through Sephadex G-25 equilibrated in PBS at 4°C. The conjugate was then sterile filtered through a 0.2- μ m filter.

The generation of cAC10 antibody-drug conjugates with two and four MMAE molecules per antibody, E2 and E4, respectively, involved a partial reduction of the mAb followed by reaction with Val-Cit-MMAE. The antibody cAC10 (10 mg/mL) was partially reduced by addition of DTT to a final

DTT:mAb molar ratio of 3.0 followed by incubation at 37°C for ~2 hours. The reduction reaction was then chilled to ~10°C and the reduced cAC10 purified away from excess DTT via diafiltration. After diafiltration, the thiol concentration in the partially reduced cAC10 was determined by DTNB; in this manner, an average of approximately two disulfide bonds were reduced, thus exposing approximately four reduced Cys:mAb. To conjugate all of the reduced Cys, Val-Cit-MMAE was added to a final Val-Cit-MMAE:reduced Cys molar ratio of ~1.15. The conjugation reaction was carried out in the presence of 15% v/v of DMSO and allowed to proceed at ~10°C for ~30 minutes. After the conjugation reaction, excess free Cys (2 mol/L Cys per mol/L Val-Cit-MMAE) was added to quench unreacted Val-Cit-MMAE to produce the Cys-Val-Cit-MMAE adduct. The Cys quenching reaction was allowed to proceed at ~10°C for ~30 minutes. The Cys-quenched reaction mixture was purified and buffer-exchanged into PBS by diafiltration to obtain the partially loaded cAC10-Val-Cit-MMAE referred to as E4-Mixture.

Preparative Hydrophobic Interaction Chromatography Fractionation.

All chromatographic steps were performed at room temperature. A 1.6 \times 25-cm column (~50 mL) was packed with Toyopearl Phenyl-650M HIC resin (Tosoh Bioscience, Montgomeryville, PA) and equilibrated with >5 column volumes of buffer A [50 mmol/L sodium phosphate, 2 mol/L NaCl (pH 7.0)]. To prepare the sample for loading onto the column, 39 mL of E4-Mixture (12.9 mg/mL) were mixed with an equivalent volume of buffer A' [50 mmol/L sodium phosphate, 4 mol/L NaCl (pH 7.0)]. After sample loading, the column was washed with buffer A until an $A_{280\text{ nm}}$ baseline was achieved. E2 was eluted and collected with a step gradient consisting of 65% buffer A/35% buffer B [80% v/v 50 mmol/L sodium phosphate (pH 7.0), 20% v/v acetonitrile]. After baseline was again achieved, E4 was eluted and collected with a step gradient consisting of 30% buffer A/70% buffer B. Both E2 and E4 peaks were collected to ~20% of their respective peak heights. The fractions of interest were buffer exchanged into PBS using Ultrafree-15 centrifugal filter devices with a molecular weight cutoff of M_r 30,000 (Millipore, Billerica, MA).

Analysis of Conjugates. Analysis of the conjugates was accomplished by hydrophobic interaction chromatography-high-performance liquid chromatography using an Ether-5PW column (Tosoh Bioscience, Montgomeryville, PA). The method consisted of a linear gradient from 100% buffer A to 100% buffer C [80% v/v 50 mmol/L sodium phosphate (pH 7.0), 10% v/v acetonitrile, 10% v/v isopropanol] in 50 minutes. The flow rate was set at 1 mL/min, the temperature was set at 30°C, and detection was followed at both 248 and 280 nm. The identity of unmodified cAC10 and E8 peaks was confirmed by injection of cAC10 and E8 standards. Because the antibody and drug have distinct absorbance maxima ($\lambda_{\text{max}} = 280$ and 248 nm, respectively), it was possible to identify peaks corresponding to cAC10 conjugates with two, four, and six drugs per antibody by overlaying peak spectra.

Additional confirmation of the identity of purified E2 and E4 was accomplished by UV-VIS analysis. The absorbance at 280 nm of the drug and the antibody contribute to the total absorbance ($A_{280\text{ nm}}$):

$$A_{280} = \epsilon_D^{280} C_D l + \epsilon_{Ab}^{280} C_{Ab} l \quad (1)$$

where

ϵ_D^{280} = extinction coefficient of the drug at 280 nm,

ϵ_{Ab}^{280} = extinction coefficient of the mAb at 280 nm,

C_D = concentration of the drug,

C_{Ab} = concentration of the mAb, and

l = detector path length; and an analogous equation for the total absorbance at 248 nm:

$$A_{248} = \epsilon_D^{248} C_D l + \epsilon_{Ab}^{248} C_{Ab} l \quad (2)$$

Dividing equation 2 by equation 1 and rearranging:

$$MR = \frac{\epsilon_{Ab}^{248} - R\epsilon_{Ab}^{280}}{R\epsilon_D^{280} - \epsilon_D^{248}} \quad (3)$$

where

$MR = C_D/C_{Ab}$ = Drug:mAb molar ratio

$R = A_{248}/A_{280}$ = Absorbance ratio.

The drug:mAb molar ratio was then calculated using equation 3 and extinction coefficients of the drug ($\epsilon_D^{248} = 1.5 \times 10^3$ L/mol · cm and $\epsilon_D^{280} = 1.59 \times 10^4$ L/mol · cm) and mAb ($\epsilon_{Ab}^{248} = 9.413 \times 10^4$ L/mol · cm and $\epsilon_{Ab}^{280} = 2.3415 \times 10^5$ L/mol · cm).

In vitro Characterization of cAC10-Val-Cit-MMAE Antibody-Drug Conjugates. Competition binding was performed on the antibody-drug conjugates to determine whether the conjugation process or presence of drug impaired the antigen binding. To compare saturation binding of mAb and antibody-drug conjugate, 5×10^5 Karpas-299 cells were combined with serial dilutions of cAC10, E2, E4, or E8 in the presence of 1 μ g/mL cAC10 labeled with Alexa Fluor 488 (Molecular Probes, Eugene, OR) in staining medium for 30 minutes on ice then washed twice with ice-cold staining medium. Labeled cells were measured using a Fusion microplate reader (Perkin-Elmer, Boston, MA). Sample data were baseline corrected and reported as the percentage of maximum fluorescence as calculated by the sample fluorescence divided by the fluorescence of cells stained with 1 μ g/mL cAC10-Alexa Fluor 488 alone.

The growth inhibitory activities of cAC10 conjugates were determined by measuring DNA synthesis. Conjugates were incubated with CD30⁺ Karpas-299 or L540cy cells or CD30⁻ WSU-NHL cells. After a 92-hour incubation with cAC10 or cAC10 antibody-drug conjugates, cells were labeled with [³H]thymidine, 0.5 μ Ci/well, for 4 hours at 37°C. Cells were harvested onto filters using a harvester, mixed with scintillation fluid, and the radioactivity was measured with a Topcount scintillation counter (Packard Instruments, Meriden, CT). The percent radioactivity incorporation relative to untreated controls was plotted *versus* concentration for each molecule. The data were fit to a sigmoidal dose-response curve (variable slope) with Prism 4.01 software (GraphPad Software, Inc., San Diego, CA) to determine the IC₅₀ (defined as the mAb concentration that gave 50% inhibition of DNA synthesis).

Xenograft Models of Human Anaplastic Large-Cell Lymphoma. To establish a s.c. disease model of anaplastic large-cell lymphoma, 5×10^6 Karpas-299 cells were implanted into the right flank of C.B-17 SCID mice (Harlan, Indianapolis, IN). Therapy with antibody-drug conjugates was initiated when the tumor size in each group of 6 to 10 animals averaged 90 and

100 mm³ for the single-dose and multidose experiments, respectively. Treatment consisted of either a single injection or multiple i.v. injections using the schedule of one injection every 4 days for 4 injections (q4d \times 4). Tumor volume was calculated using the formula (length \times width²)/2. A tumor that decreased in size such that it was impalpable was defined as a complete regression. A complete regression that lasted >100 days after tumor implant was defined as a cure. Animals were euthanized when tumor volumes reached \sim 1000 mm³. Pairwise treatment groups were compared using Kaplan-Meier analysis for survival with Prism 4.01 software.

Maximum-Tolerated Dose (MTD). Groups of three BALB/c mice (Harlan) received injections of 30 to 60 mg/kg E8, 60 to 120 mg/kg E4, or 200 to 250 mg/kg E2 via the tail vein to determine the single-dose MTD. Mice were monitored daily for 14 days, and both weight and clinical observations were recorded. Mice that developed significant signs of distress were sacrificed in accordance with Institutional Animal Care and Use Committee guidelines. The MTD was defined as the highest dose that did not cause serious overt toxicities or >20% weight loss in any of the animals.

Pharmacokinetics. The pharmacokinetics of cAC10, E2, E4, and E8 were evaluated in SCID mice. SCID mice ($n = 3$) were administered 10 mg/kg test material (based on the antibody component) by tail vein injection. Blood samples were collected from each mouse via the saphenous vein at 1 hour, 4 hours, 1 day, 2 days, 4 days, 7 days, 14 days, 21 days, 28 days, 35 days, 42 days, and 49 days after injection. Blood was collected into heparin coated tubes followed by centrifugation (14,000 \times g, 3 minutes) to isolate plasma. Plasma concentrations of cAC10 and antibody-drug conjugates were measured by ELISA.

Briefly, the ELISA consisted of the following steps: plate coat, block, sample binding, secondary mAb, 3,3',5,5'-tetramethylbenzidine dihydrochloride, and acid quench. After each step, the wells were washed with wash buffer [PBS, 0.05% Tween 20 (pH 7.4)] three times. In the plate coat step, anti-cAC10 mAb was coated onto 96-well plates at 2 μ g/mL in carbonate buffer [0.1 mol/L carbonate/bicarbonate (pH 9.6)] at 4°C overnight. After the plate coat, blocking buffer (PBS, 1% BSA, 0.05% Tween 20) was added and incubated at room temperature for 1 hour. Next, 100 μ L of standard or diluted plasma sample were added to triplicate wells for 1 hour at room temperature. The secondary step consisted of a mouse anti-human IgG-horseradish peroxidase conjugate (Southern Biotech, Birmingham, AL) incubated for 1 hour. Subsequently, 100 μ L of 3,3',5,5'-tetramethylbenzidine (Sigma, St. Louis, MO) were added to each well, and upon color development, the reaction was stopped with 100 μ L of 1 N sulfuric acid. Absorbance was measured using a VMax Kinetic Microplate reader (Molecular Devices, Sunnyvale, CA) at 450 nm and a blank at 630 nm. Noncompartmental pharmacokinetic parameters were calculated with WinNonlin (Pharsight, Mountain View, CA).

RESULTS

Generation of Antibody-Drug Conjugate with Reduced Drug Loading. Our previous studies demonstrated that an anti-CD30 antibody-drug conjugate containing eight MMAE drug molecules per mAb (referred to here as E8) had potent and

specific cytotoxic activity against CD30 expressing cells both *in vitro* and *in vivo* (12, 13). This antibody-drug conjugate was constructed by reducing the four interchain disulfide bonds of cAC10 and conjugating Val-Cit-MMAE to the eight exposed sulfhydryls. To evaluate the effect of drug loading on the activity of cAC10 antibody-drug conjugates, conjugates with two and four MMAE molecules per mAb, E2 and E4, respectively, were constructed. cAC10 was partially reduced with DTT to yield an average of four reactive sulfhydryls per mAb. The partially reduced mAb was then mixed with reactive Val-Cit-MMAE to generate cAC10-Val-Cit-MMAE with an average molar ratio of 4.0 to 4.2 MMAE molecules per antibody, referred to as E4-Mixture. As determined by hydrophobic interaction chromatography–high-performance liquid chromatography (Fig. 1A), the resulting product was a mixture of species that were identified as cAC10, cAC10 conjugated with two molecules of MMAE (E2), four molecules of MMAE (E4), six molecules of MMAE (E6), and eight molecules of MMAE (E8). The five major peaks can be positively identified because attachment of drug results in greater absorbance at ~ 248 nm (λ_{\max} for drug) relative to 280 nm (λ_{\max} for cAC10; Fig. 1A, insert). This partially loaded antibody-drug conjugate mixture contained $\sim 9\%$ unconjugated cAC10, 22% E2, 30% E4, 23% E6, and 9% E8. Upon preparative hydrophobic interaction chromatography fractionation, E2 (Fig. 1B) and E4 (Fig. 1C) were found to be $>95\%$ pure by analytical hydrophobic interaction chromatography–high-performance liquid chromatography. Additional confirmation of the identity of E2 and E4 was obtained by UV-VIS analysis using extinction coefficients of the drug and antibody (see Materials and Methods), resulting in drug to mAb molar ratios of 2.0 and 4.0 for E2 and E4, respectively. Production of E8 was described previously and the molar ratio was determined to be 8.0 (13). For studies described herein the concentrations of antibody-drug conjugates are reported based on the mAb component.

***In vitro* Characterization.** Competition binding experiments were performed to determine whether conjugation of MMAE to cAC10 interferes with the CD30 binding capability of the antibody-drug conjugates. CD30⁺ Karpas-299 cells were incubated with 1 $\mu\text{g}/\text{mL}$ fluorescently labeled cAC10 combined with serial dilutions of unlabeled antibody, E2, E4, or E8. Each of the antibody-drug conjugate variants effectively competed with fluorescently labeled cAC10 equivalent to unlabeled cAC10 as shown in Fig. 2. Thus, conjugation with MMAE did not reduce the CD30 binding capabilities of the cAC10 antibody-drug conjugates.

The *in vitro* cytotoxic activities of the antibody-drug conjugates were evaluated by a [³H]thymidine incorporation assay with CD30⁺ Karpas-299 and L540cy cells and CD30⁻ WSU-NHL cells. E8 demonstrated significant activity against the Karpas-299 cells with an IC_{50} of 1.0 ng/mL (Fig. 3A). Decreasing the amount of drug in half to four MMAE molecules per mAb (E4) increased the IC_{50} to 2.9 ng/mL. Halving the drug loading again additionally increased the IC_{50} to 6.2 ng/mL with E2. Against the Hodgkin's disease line L540cy, the antibody-drug conjugates had a similar trend with IC_{50} values of 1.4, 4.5, and 9.2 ng/mL for E8, E4, and E2, respectively (Fig. 3B). Selectivity of the antibody-drug conjugates was evaluated with CD30⁻ WSU-NHL cell line, which was insensitive to all cAC10-

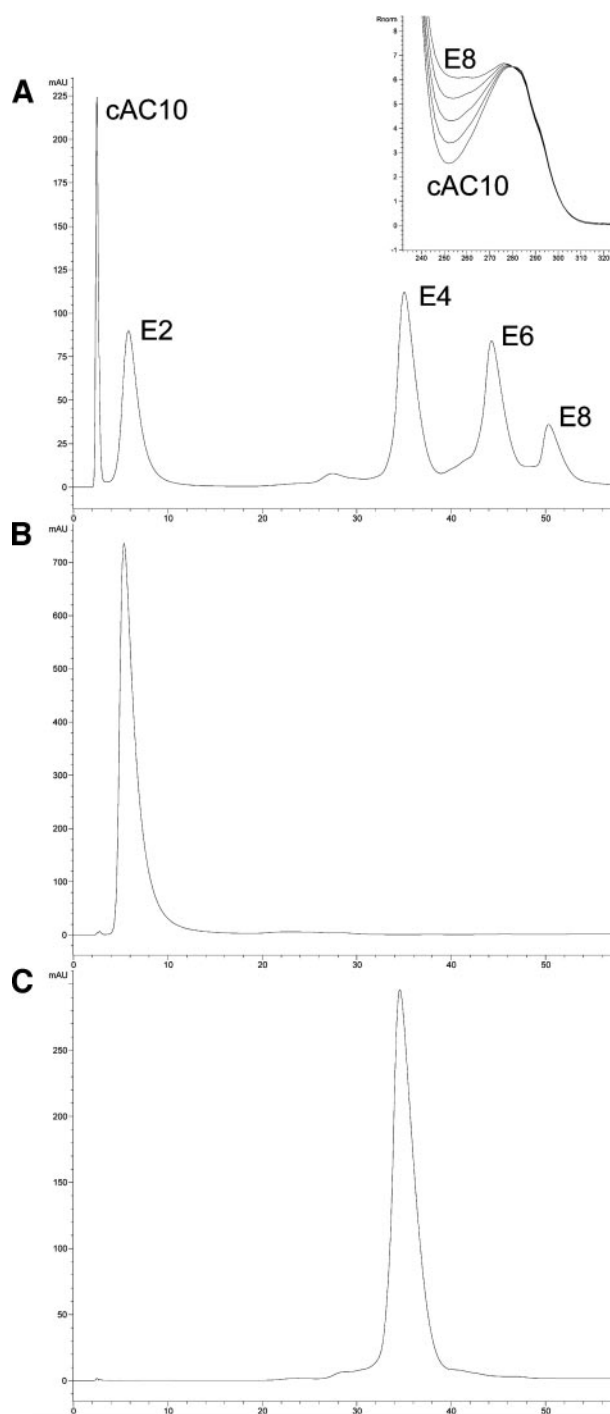


Fig. 1 Hydrophobic interaction chromatography–high-performance liquid chromatography chromatograms of partially loaded E4-Mixture (A), E2 (B), and E4 (C). The insert in A shows an overlay of UV spectra corresponding to peaks cAC10, E2, E4, E6, and E8.

antibody-drug conjugates with IC_{50} values > 1000 ng/mL (data not shown).

Xenograft Models of Human Anaplastic Large-Cell Lymphoma. The effect of drug loading on *in vivo* antitumor activity was evaluated in SCID mice with human Karpas-299

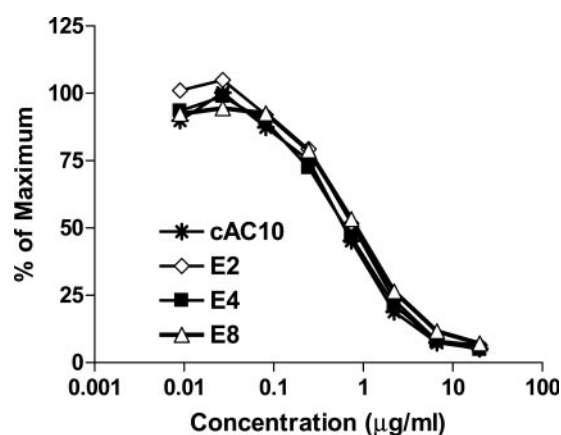


Fig. 2 CD30⁺ Karpas-299 cells were combined with 1 µg/mL fluorescently labeled cAC10 and serial dilutions of either cAC10, E2, E4, or E8 from 20 µg/mL to 9 ng/mL. The labeled cells were washed with staining media and the fluorescence was measured. The normalized fluorescence intensities were plotted versus mAb concentration as described in Materials and Methods.

s.c. xenografts. Therapy was administered every fourth day for a total of four injections (q4d×4), starting when tumor volumes reached 50 to 100 mm³. Using this schedule, we previously found that E8 at 1 mg/kg produced 100% complete regressions (13). At the same dose level, E4 also led to 100% complete regressions (data not shown). With the goal of comparing the activity of the antibody-drug conjugates, lower doses were used for E4 and E8. Cohorts of mice bearing s.c. Karpas-299 xenografts were treated with multiple doses of E4 or E8 at 0.25 or 0.5 mg/kg/dose. Although E8 had twice the amount of MMAE as E4 at the same mAb dose, they were equally effective at 0.5 mg/kg ($P = 0.36$; Table 1 and Fig. 4A). At a 0.5 mg/kg/dose, 5 of the 10 animals treated with E4 achieved complete regressions, and E8 induced 6 of 10 complete regressions. At 0.25 mg/kg/dose, both of these antibody-drug conjugates induced a similar delay in tumor growth compared with untreated control animals but no complete regressions. Unexpectedly, E2 at 1.0 mg/kg/dose, which contained the same amount of MMAE as E4 at 0.5 mg/kg/dose and E8 at 0.25 mg/kg, gave the best therapeutic response with 10 of 10 cures. A physical mixture of the drug MMAE with cAC10, equivalent to E8 at the 0.5 mg/kg dose, produced only a slight delay in tumor growth compared with untreated ($P = 0.1$), highlighting that the linkage of drug to antibody is critical for achieving antitumor activity.

To additionally compare antibody-drug conjugate with different drug loading, single-dose treatments with E2, E4, and E8 in this same model were then compared at 0.5 and 1.0 mg/kg (Table 1 and Fig. 4B). At the low dose of 0.5 mg/kg, there was a marginal delay in tumor growth in animals dosed with the antibody-drug conjugates compared with untreated. Any difference between E2, E4, and E8 was minimal at 0.5 mg/kg, with zero, one, and two cures, respectively. Treatment at the 1 mg/kg dose produced significant responses with cures in all treatment groups. Cures were obtained in five of six animals treated with 1 mg/kg E8. Of the six animals treated with 1 mg/kg E4 all achieved complete regressions with five cures out to 108 days,

the end of the study (one animal was found dead on day 72 with no sign of tumor mass). Although E2 at 1.0 mg/kg contained half as much MMAE as E4, four of six mice achieved complete regressions. A physical mixture consisting of 1 mg/kg cAC10

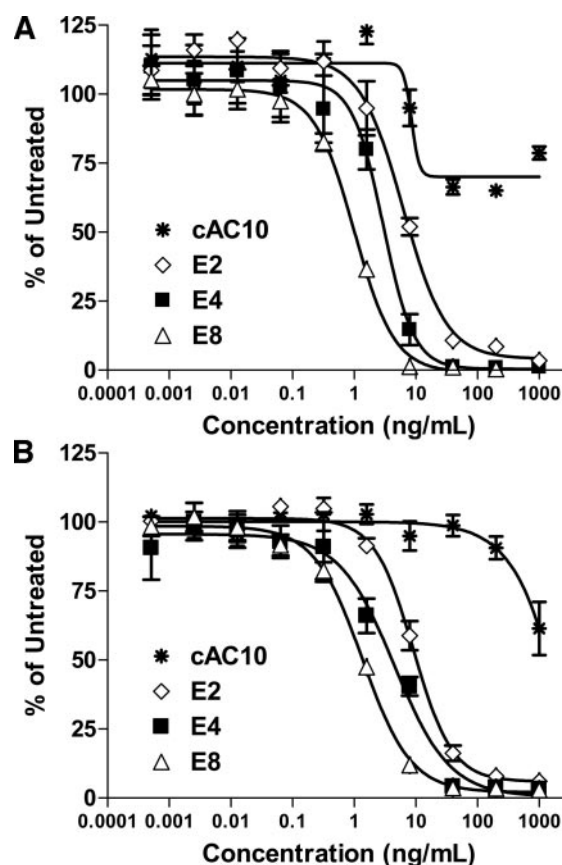


Fig. 3 Karpas-299 (A) and L540cy (B) cells were incubated with serial dilutions of cAC10 and cAC10 antibody-drug conjugates. After a 96 h incubation with the samples, [³H]thymidine was added, and its incorporation was measured. The radioactivity of the treated samples were normalized to the untreated controls and plotted versus concentration.

Table 1 Antitumor activity of E2, E4, and E8 in a s.c. Karpas-299 xenograft model

Schedule	Antibody-drug conjugate	Dose (mg/kg)	Complete regressions	Cures
q4d×4	E2	0.5	0/10	0/10
		1.0	10/10	10/10
	E4	0.25	1/10	1/10
		0.50	5/10	3/10
	E8	0.25	0/10	0/10
		0.50	6/10	6/10
×1	E2	0.5	0/6	0/6
		1.0	4/6	4/6
	E4	0.5	1/6	1/6
		1.0	6/6	5/6*
	E8	0.5	2/6	2/6
		1.0	5/6	5/6

* One mouse with a cure was found dead on day 72 with no sign of tumor mass.

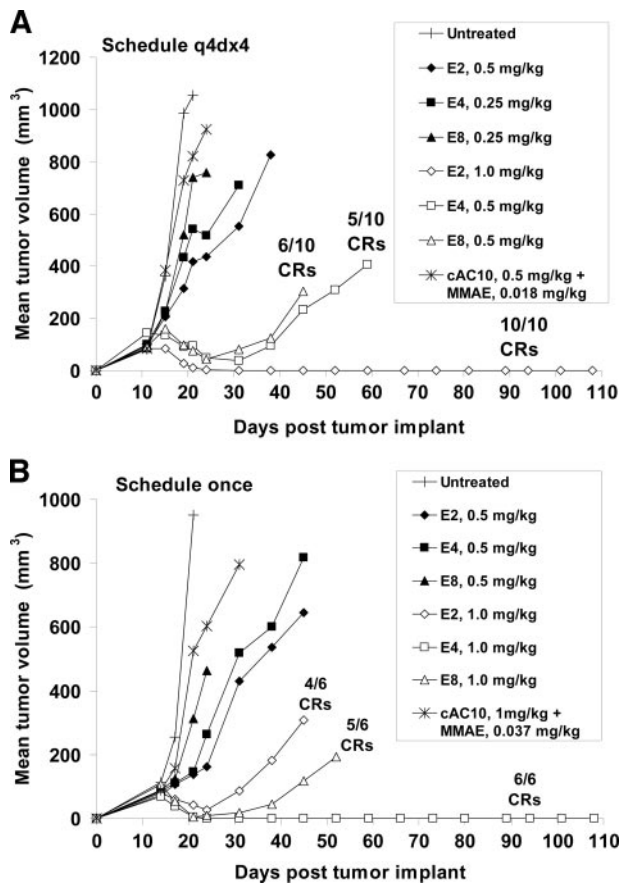


Fig. 4 Multidose and single-dose antibody-drug conjugate efficacy of SCID mice bearing s.c. xenografts. **A.** SCID mice bearing Karpas-299 s.c. tumors were injected with E2 at 0.5 or 1.0 mg/kg every 4 days for four injections. E4 and E8 were dosed at either 0.25 or 0.5 mg/kg every 4 days for four injections. **B.** SCID mice with Karpas-299 s.c. tumors were treated with a single dose of E2, E4, or E8 at 1.0 mg/kg.

plus 0.037 mg/kg free MMAE, equivalent to the amount of drug contained in 1 mg/kg E8, had little effect on tumor growth compared with untreated mice.

MTD and Therapeutic Index. The single-dose tolerability of E2, E4, and E8 was evaluated in BALB/c mice, the immunocompetent parent strain of SCID mice. The MTD was defined as the highest dose that did not induce >20% weight loss, severe signs of distress, or overt toxicities in any of the animals. For E8, mice were dosed at 10 mg/kg intervals from 30 to 60 mg/kg. At a dose of 50 mg/kg, mice had a maximum weight loss of 14% 6 days after injection, after which the weight loss was recovered. A dose of 60 mg/kg induced 23% weight loss 6 days postinjection in one animal. With E4 at 100 mg/kg animals had minimal weight loss, whereas at 120 mg/kg E4, one animal displayed signs of significant distress and 17% weight loss, and the animal was euthanized. Mice treated with E2 at doses up to 250 mg/kg, the highest dose tested, experienced a maximum weight loss of 10.5% 6 days postinjection, with no signs of distress. On the basis of these results, the MTD of E8 was 50 mg/kg, for E4 it was 100 mg/kg, and for E2 was at least 250 mg/kg. Therapeutic index, as defined by the ratio of the

single-dose MTD to the multidose dose achieving >50% complete regressions, were 100 for E8, 200 for E4, and at least 250 for E2.

Pharmacokinetics. SCID mice were treated with cAC10, E2, E4, and E8 to determine how drug loading effects pharmacokinetics (Fig. 5). Table 2 illustrates the pharmacokinetic parameters established by noncompartmental analysis. The time-concentration curves of cAC10, E2, E4, and E8 appeared to follow bi-exponential declines. The terminal half-lives were 16.7, 16.9, 14.0, and 14.7 days, respectively, and thus did not directly correlate with drug loading. However, the exposure of antibody-drug conjugates as determined by the area under the curve increased as drug loading decreased, ranging from 2638 $\mu\text{g}\cdot\text{day}/\text{mL}$ for unmodified cAC10 to 520 $\mu\text{g}\cdot\text{day}/\text{mL}$ for E8. Clearance values increased from 3.8 mL/day/kg for cAC10 to 4.4, 6.0, and 19.2 mL/day/kg as drug loading increased for E2, E4, and E8, respectively. Similarly, the volume of distribution was found to correlate with drug loading.

DISCUSSION

The effects of drug multiplicity on the *in vitro* activities of a few other antibody-drug conjugates have been reported. For example, doxorubicin-antibody-drug conjugates displayed a correlation between drug loading and cell cytotoxicity *in vitro* (20, 26). The use of branched linkers increased molar ratios as high as 16 doxorubicin molecules per mAb, which additionally

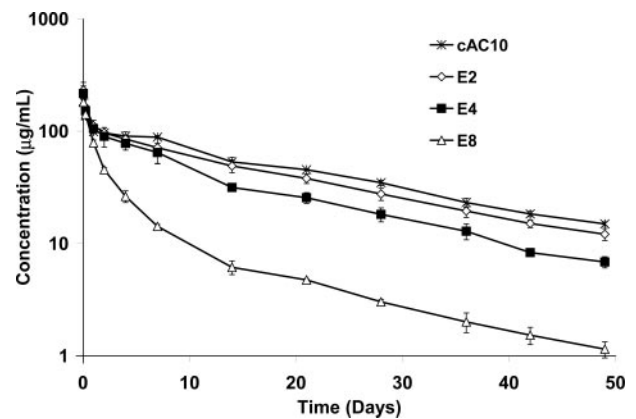


Fig. 5 Pharmacokinetics of cAC10 and cAC10-antibody-drug conjugates. SCID mice were injected via the tail vein with 10 mg/kg cAC10, E2, E4, and E8. Plasma samples were analyzed by ELISA to determine the antibody or antibody-drug conjugate concentration.

Table 2 Pharmacokinetic parameters of cAC10 and cAC10 antibody-drug conjugates in SCID mice at a dose of 10 mg/kg (\pm SD)

Name	Half-time (days)	Area under the curve ($\mu\text{g}\cdot\text{day}/\text{mL}$)	Clearance (mL/day/kg)	Volume of distribution (mL/kg)
cAC10	16.7 (0.2)	2638 (64)	3.8 (0.1)	91 (3.2)
E2	16.9 (1.7)	2313 (282)	4.4 (0.6)	107 (14)
E4	14.0 (2.5)	1689 (187)	6.0 (0.6)	122 (30)
E8	14.9 (1.8)	520 (21)	19.2 (0.8)	414 (66)

improved the *in vitro* potency without affecting antigen binding (20). The activities of TA.1-maytansinoid conjugates with an average ranging from one to six drugs per mAb were compared *in vitro*, and optimal cytotoxicity was achieved with an average of four drugs per mAb (16). Here, we described how drug multiplicity affects both the *in vitro* and *in vivo* characteristics of antibody-drug conjugates produced with MMAE.

Attaching a drug to a mAb can be accomplished through a variety of approaches, including lysine, aldehyde, or, as we have used here, cysteine chemistries. IgG1 molecules contain 12 intrachain and 4 interchain disulfide bonds. However, it has been shown that the latter are significantly more susceptible to reduction by agents such as DTT than are the intrachain bonds (27, 28). In fact, Willner *et al.* (27) reported that reduction of a chimeric antibody with up to 100 molar equivalents of DTT could only generate eight sulfhydryls per antibody corresponding to reduction of the four interchain disulfide bonds. Using lower concentrations of DTT, the reducing conditions that we used here in preparation of the fully and partially loaded antibody-drug conjugate yielded 8 and 4 thiols/mAb, respectively. Fully loaded E8 thus has one MMAE molecule attached to each cysteine that comprises the interchain disulfides of a mAb. Partially loaded E2 and E4 can theoretically occupy any two or four of these locations, respectively. It is not known if there is preferential localization of the drugs to the heavy/light chain or hinge disulfide bonds. Given that the partial reduction process described here results in production of antibody-drug conjugates with only even numbers of MMAE per antibody as shown in Fig. 1A and subsequent characterization (data not shown), it is likely that localization of drugs occurs simultaneously at both cysteine residues of a disulfide bond.

Competition binding experiments revealed that loading cAC10 with two, four, or eight drugs per antibody had no measurable effect on the binding to the target antigen CD30 (Fig. 2). On the basis of the IC₅₀ values, E4 was 3-fold less potent than E8, and the E2 was 2-fold less potent than E4 for both CD30⁺ cell lines tested. Similar to doxorubicin-antibody-drug conjugates (20, 26), the *in vitro* potency of the cAC10-antibody-drug conjugates was directly dependent on drug loading and thus the total MMAE exposure.

E4 demonstrated antitumor activity comparable with E8 in a Karpas-299 xenograft model at the same antibody dose, half the MMAE dose. On the basis of the *in vitro* finding that potency was directly related to drug loading, an equivalent *in vivo* antitumor activity of E4 and E8 was anticipated. Investigation of the pharmacokinetics of the antibody-drug conjugates revealed that clearance was dependent on drug loading of the antibody-drug conjugates and exposure (area under the curve) was inversely related to drug loading. The 3-fold larger area under the curve, and thus increased tumor exposure, of E4 compared with E8 was apparently sufficient to compensate for reduced potency, leading to equivalent efficacy. Attempts to improve efficacy by decelerating the plasma elimination half-life to augment area under the curves have been accomplished by methods including the construction of albumin fusion proteins for IFN α (29) and liposomal delivery of the anticancer drug lurtotecan (30). Unlike these examples where the objective was to lengthen the plasma half-life, the enhanced exposure of E4 was a valuable unexpected consequence of reducing MMAE

loading. Although the concentrations reported here are based on the antibody component it has been observed that MMAE is released from the antibody-drug conjugate over time *in vivo*.¹

Dosing E2 with 1.0 mg/kg/dose q4d \times 4 yielded 10 of 10 cures, an improved antitumor effect compared with E4 and E8 at 0.5 mg/kg/dose ($P = 0.0012$ and $P = 0.0289$, respectively). Although E2 did not demonstrate equivalent antitumor activity compared with E4 ($P < 0.0001$) at the same mAb dose (0.5 mg/kg, q4d \times 4), the dose of E2 needed to achieve equivalent antitumor activity compared with E4 is probably <2 -fold based on the *in vivo* efficacy experiments. Similar to E4, the improved exposure of E2 may play a significant part in compensating for the lower *in vitro* potency.

To maximize the therapeutic potential of cAC10-Val-Cit-MMAE antibody-drug conjugates, a high therapeutic index is needed. Reducing the amount of MMAE molecules per mAb from eight to four enhanced the therapeutic index 2-fold. Additional studies are under way to determine whether the target organ toxicities of E2, E4, and E8 are different or if the MTD is simply due to the presence of the total amount of drug in the system. Given the steep dose-response curves of chemotherapeutic reagents, a 2-fold difference in therapeutic index is significant and should translate into improvements in therapeutic efficacy.

By reducing the quantity of MMAE from eight to four molecules per mAb, we reported a decrease of *in vitro* activity, yet more importantly, demonstrated equivalent antitumor activity *in vivo*. Although an additional reduction in drug loading to two MMAE molecules per antibody further reduced the *in vitro* activity, E2 had equivalent or better efficacy than E4 and E8 at double the dose in a multidose setting. The therapeutic index was increased 2-fold by reducing drug loading from eight MMAE molecules to four and, at the very least, maintained with a further reduction to two drugs per antibody. In summary, there is considerable value in optimizing drug substitution of antibody-drug conjugates that may lead to enhanced product candidates such as the anti-CD30 antibody-drug conjugate described here.

REFERENCES

1. Carter P. Improving the efficacy of antibody-based cancer therapies. *Nat Rev Cancer* 2001;1(2):118–29.
2. Shields RL, Lai J, Keck R, et al. Lack of fucose on human IgG1 N-linked oligosaccharide improves binding to human Fc γ RIII and antibody-dependent cellular toxicity. *J Biol Chem* 2002;277(30):26733–40.
3. Shinkawa T, Nakamura K, Yamane N et al. The absence of fucose but not the presence of galactose or bisecting *N*-acetylglucosamine of human IgG1 complex-type oligosaccharides shows the critical role of enhancing antibody-dependent cellular cytotoxicity. *J Biol Chem* 2003;278(5):3466–73.
4. Pastan I, Kreitman RJ. Immunotoxins in cancer therapy. *Curr Opin Investig Drugs* 2002;3(7):1089–91.

¹ R. J. Sanderson, M. A. Hering, M. M. C. Sun, A. W. Siadak, P. D. Senter, and A. F. Wahl. *In vivo* drug-linker stability of cAC10-vcMMAE, an anti-CD30 dipeptide-linked monomethyl auristatin E immunconjugate, submitted for publication.

5. Juweid ME. Radioimmunotherapy of B-cell non-Hodgkin's lymphoma: from clinical trials to clinical practice. *J Nucl Med* 2002;43(11):1507-29.
6. Cheson BD. Radioimmunotherapy of non-Hodgkin lymphomas. *Blood* 2003;101(2):391-8.
7. Saleh MN, Sugarman S, Murray J, et al. Phase I trial of the anti-Lewis Y drug immunoconjugate BR96-doxorubicin in patients with Lewis Y-expressing epithelial tumors. *J Clin Oncol* 2000;18(11):2282-92.
8. Sievers EL, Larson RA, Stadtmauer EA, et al. Efficacy and safety of gemtuzumab ozogamicin in patients with CD33-positive acute myeloid leukemia in first relapse. *J Clin Oncol* 2001;19(13):3244-54.
9. Tolcher AW, Ochoa L, Hammond LA, et al. Cantuzumab mertansine, a maytansinoid immunoconjugate directed to the CanAg antigen: a phase I, pharmacokinetic, and biologic correlative study. *J Clin Oncol* 2003;21(2):211-22.
10. Bross PF, Beitz J, Chen G, et al. Approval summary: gemtuzumab ozogamicin in relapsed acute myeloid leukemia. *Clin Cancer Res* 2001;7(6):1490-6.
11. Chan SY, Gordon AN, Coleman RE, et al. A phase 2 study of the cytotoxic immunoconjugate CMB-401 (hCTM01-calicheamicin) in patients with platinum-sensitive recurrent epithelial ovarian carcinoma. *Cancer Immunol Immunother* 2003;52(4):243-8.
12. Doronina SO, Toki BE, Torgov MY, et al. Development of potent and highly efficacious monoclonal antibody auristatin conjugates for cancer therapy. *Nat Biotechnol* 2003;21(7):778-84.
13. Francisco JA, Cerveny CG, Meyer DL, et al. cAC10-vcMMAE, an anti-CD30-monomethyl auristatin E conjugate with potent and selective antitumor activity. *Blood* 2003;102:1458-65.
14. Chari RV, Jackel KA, Bourret LA, et al. Enhancement of the selectivity and antitumor efficacy of a CC-1065 analogue through immunoconjugate formation. *Cancer Res* 1995;55(18):4079-84.
15. Meyer DL, Senter PD. Recent advances in antibody drug conjugates for cancer therapy, Chp 23. *Annu Rep Med Chem* 2003;38:229-37.
16. Chari RV, Martell BA, Gross JL, et al. Immunoconjugates containing novel maytansinoids: promising anticancer drugs. *Cancer Res* 1992;52(1):127-31.
17. Dubowchik GM, Firestone RA, Padilla L, et al. Cathepsin B-labile dipeptide linkers for lysosomal release of doxorubicin from internalizing immunoconjugates: model studies of enzymatic drug release and antigen-specific in vitro anticancer activity. *Bioconjug Chem* 2002;13(4):855-69.
18. Hamann PR, Hinman LM, Hollander I, et al. Gemtuzumab ozogamicin, a potent and selective anti-CD33 antibody-calicheamicin conjugate for treatment of acute myeloid leukemia. *Bioconjug Chem* 2002;13(1):47-58.
19. Hamann PR, Hinman LM, Beyer CF, et al. An anti-CD33 antibody-calicheamicin conjugate for treatment of acute myeloid leukemia. Choice of linker. *Bioconjug Chem* 2002;13(1):40-6.
20. King HD, Yurgaitis D, Willner D, et al. Monoclonal antibody conjugates of doxorubicin prepared with branched linkers: a novel method for increasing the potency of doxorubicin immunoconjugates. *Bioconjug Chem* 1999;10(2):279-88.
21. Schwab U, Stein H, Gerdes J, et al. Production of a monoclonal antibody specific for Hodgkin and Sternberg-Reed cells of Hodgkin's disease and a subset of normal lymphoid cells. *Nature (Lond.)* 1982;299(5878):65-7.
22. Stein H, Mason DY, Gerdes J, et al. The expression of the Hodgkin's disease associated antigen Ki-1 in reactive and neoplastic lymphoid tissue: evidence that Reed-Sternberg cells and histiocytic malignancies are derived from activated lymphoid cells. *Blood* 1985;66(4):848-58.
23. Gerdes J, Schwarting R, Stein H. High proliferative activity of Reed Sternberg associated antigen Ki-1 positive cells in normal lymphoid tissue. *J Clin Pathol (Lond.)* 1986;39(9):993-7.
24. Horie R, Watanabe T. CD30: expression and function in health and disease. *Semin Immunol* 1998;10(6):457-70.
25. Wahl AF, Klussman K, Thompson JD, et al. The anti-CD30 monoclonal antibody SGN-30 promotes growth arrest and DNA fragmentation in vitro and affects antitumor activity in models of Hodgkin's disease. *Cancer Res* 2002;62(13):3736-42.
26. Firestone RA, Willner D, Hofstead SJ, et al. Synthesis and antitumor activity of the immunoconjugate BR96-Dox. *J Control Release* 1996;39:251-9.
27. Willner D, Trail PA, Hofstead SJ, et al. (6-Maleimidocaproyl)hydrazide of doxorubicin: a new derivative for the preparation of immunoconjugates of doxorubicin. *Bioconjug Chem* 1993;4(6):521-7.
28. Schroeder DD, Tankersley DL, Lundblad JL. A new preparation of modified immune serum globulin (human) suitable for intravenous administration. I. Standardization of the reduction and alkylation reaction. *Vox Sang* 1981;40(6):373-82.
29. Osborn BL, Olsen HS, Nardelli B, et al. Pharmacokinetic and pharmacodynamic studies of a human serum albumin-interferon-alpha fusion protein in cynomolgus monkeys. *J Pharmacol Exp Ther* 2002;303(2):540-8.
30. Emerson DL, Bendele R, Brown E, et al. Antitumor efficacy, pharmacokinetics, and biodistribution of NX 211: a low-clearance liposomal formulation of lurtotecan. *Clin Cancer Res* 2000;6(7):2903-12.

Clinical Cancer Research

Effects of Drug Loading on the Antitumor Activity of a Monoclonal Antibody Drug Conjugate

Kevin J. Hamblett, Peter D. Senter, Dana F. Chace, et al.

Clin Cancer Res 2004;10:7063-7070.

Updated version Access the most recent version of this article at:
<http://clincancerres.aacrjournals.org/content/10/20/7063>

Cited articles This article cites 29 articles, 16 of which you can access for free at:
<http://clincancerres.aacrjournals.org/content/10/20/7063.full#ref-list-1>

Citing articles This article has been cited by 67 HighWire-hosted articles. Access the articles at:
<http://clincancerres.aacrjournals.org/content/10/20/7063.full#related-urls>

E-mail alerts [Sign up to receive free email-alerts](#) related to this article or journal.

Reprints and Subscriptions To order reprints of this article or to subscribe to the journal, contact the AACR Publications Department at pubs@aacr.org.

Permissions To request permission to re-use all or part of this article, use this link
<http://clincancerres.aacrjournals.org/content/10/20/7063>.
Click on "Request Permissions" which will take you to the Copyright Clearance Center's (CCC) Rightslink site.